

Nanoscale topographic pattern formation on Kr^+ -bombarded germanium surfaces

Joy C. Perkinson, Charbel S. Madi, and Michael J. Aziz^{a)}

Harvard School of Engineering and Applied Sciences, 9 Oxford Street, Cambridge, Massachusetts 02138

(Received 3 July 2012; accepted 30 January 2013; published 19 February 2013)

The nanoscale pattern formation of Ge surfaces uniformly irradiated by Kr^+ ions was studied in a low-contamination environment at ion energies of 250 and 500 eV and at angles of 0° through 80° . The authors present a phase diagram of domains of pattern formation occurring as these two control parameters are varied. The results are insensitive to ion energy over the range covered by the experiments. Flat surfaces are stable from normal incidence up to an incidence angle of $\theta = 55^\circ$ from normal. At higher angles, the surface is linearly unstable to the formation of parallel-mode ripples, in which the wave vector is parallel to the projection of the ion beam on the surface. For $\theta \geq 75^\circ$ the authors observe perpendicular-mode ripples, in which the wave vector is perpendicular to the ion beam. This behavior is qualitatively similar to those of Madi *et al.* for Ar^+ -irradiated Si but is inconsistent with those of Ziberi *et al.* for Kr^+ -irradiated Ge. The existence of a window of stability is qualitatively inconsistent with a theory based on sputter erosion [R. M. Bradley and J. M. Harper, *J. Vac. Sci. Technol. A* **6**, 2390 (1988)] and qualitatively consistent with a model of ion impact-induced mass redistribution [G. Carter and V. Vishnyakov, *Phys. Rev. B* **54**, 17647 (1996)] as well as a crater function theory incorporating both effects [S. A. Norris *et al.*, *Nat. Commun.* **2**, 276 (2011)]. The critical transition angle between stable and rippled surfaces occurs 10° – 15° above the value of 45° predicted by the mass redistribution model. © 2013 American Vacuum Society. [<http://dx.doi.org/10.1116/1.4792152>]

I. INTRODUCTION

Ion irradiation of surfaces has been shown to create ripples, dots, holes, and ultrasoothing on a variety of materials.¹ Features as small as 7 nm have been observed,² leading to interest in ion irradiation as a technique for large-scale production of devices with sublitographic features.³ It is thus of interest to develop a working model to predict and understand the behavior of surfaces under ion bombardment. Recent work with Ar^+ -irradiated Si (Ref. 6) has shown smoothing at small deviation angles θ from normal incidence, which is inconsistent with theories in which instability originates in sputter erosion.^{4,5} These results have been explained by a model with a single adjustable parameter, in which ion impact-induced mass redistribution leads to both smoothing at low incidence angles as well as instability at higher incidence angles.¹⁷ The results have also been explained using the parameter-free crater function theory of Norris *et al.*⁷ Crater function theory permits the separation of redistributive and erosive effects and, together with the experiments,¹⁷ indicates that the effect of redistribution on surface pattern formation is an order of magnitude larger than that of erosion, except possibly at the most grazing angles of incidence.^{7,8} While results have been obtained for Ar^+ irradiation of Si, much less work has been done on the irradiation of Ge. Wei *et al.* have reported that for ion irradiation energies above about 5 keV, Ge forms high aspect ratio morphologies that are qualitatively different than the patterns we observe for lower energies,^{9–13} and at 5 keV, Ge forms hole patterns that are also qualitatively different from

those formed at lower energies.^{9,13,14} Furthermore, recent work on pattern formation phase diagrams under low energy (0.5–2 keV) noble gas ion irradiation of Ge by Ziberi *et al.*¹⁵ is inconsistent with both the Bradley–Harper (BH) theory as well as the ion impact-induced mass redistribution model. This raises the question of whether Ge exhibits fundamentally different behavior than Si.

This paper describes a study of Kr^+ bombardment of Ge in a low-contamination environment similar to that employed for Si by Madi *et al.* Results reveal smoothing at low incidence angles, which is inconsistent with other published data on irradiation of Ge,¹⁵ but is qualitatively similar to the results of Madi *et al.* for Ar^+ -irradiated Si.⁶ Pattern formation or smoothing was studied within the linear regime of surface dynamics, at low fluence. The results are compiled into a phase diagram in the control parameter space of ion energy and incidence angle for Kr^+ irradiation of Ge, which contrasts with the findings of Ziberi *et al.* Finally, we discuss the observed results in the context of the erosion-based theory of BH,⁵ the ion impact-induced mass redistribution model of Carter and Vishnyakov (CV) (Ref. 16) as modified by Madi *et al.*,¹⁷ and the crater function theory of Norris *et al.*⁷

II. EXPERIMENT

Samples were made of Ge(001) (p-type, 0.4 Ω cm) and were $1 \times 1 \text{ cm}^2$ in area. Samples were affixed with molten indium hidden from the ion beam to graphite wedges that were coated with Si wafers to reduce metallic surface contamination. Wedges were of angles between 0° and 80° with respect to the ion source. Although Si shields for a Ge sample do not eliminate the possibility of composition-driven instabilities,

^{a)}Electronic mail: maziz@harvard.edu

such instabilities have been demonstrated experimentally only for surface contamination with metals. It remains for future work to prove whether or not composition-driven instabilities exist only for metals. Furthermore, Rutherford backscattering spectrometry analysis of the samples in a channeling geometry shows that any Si coverage is below the detection limit of $5 \times 10^{15}/\text{cm}^2$. Ge was then uniformly irradiated at a working pressure of 1.8×10^{-4} Torr at room temperature. Ion flux was 3×10^{15} ions/cm²/s in a plane normal to the ion beam direction. High purity Kr⁺ ions were produced at energies of 250 and 500 eV by a Veeco 3 cm RF source with graphite grids. Distance from the ion source to samples was 15 cm. In order to safely neglect nonlinearities, fluences were chosen to limit irradiation to the linear regime of surface dynamics, except where stated otherwise, as discussed in Sec. III. Unless otherwise specified, fluences reported in this paper are reckoned in a plane perpendicular to the direction of the ion beam. Measurements of temperature during sustained 250 eV Ar⁺ on Si bombardment, in the same chamber and using the same ion gun as in the present study, indicate that the substrate temperature reaches 180 °C.¹⁸ Because we use a similar experimental system, we expect substrates used in this study could also reach a comparable temperature. Previous studies by our group have noted qualitative pattern changes around 300 °C, but not at lower temperatures.¹⁹ Thus, we do not expect that temperature has played a role in the pattern formation reported here. Following irradiation, samples were imaged using atomic force microscopy (AFM). Wavelength and surface roughness were measured using WSxM software.²⁰

III. RESULTS AND DISCUSSION

Kr⁺ irradiation of Ge was conducted at ion energies of 250 and 500 eV and at incidence angles between 0° and 80°. Various surface patterns were observed, including smoothening, ripples with a wave vector parallel or perpendicular to the incident ion beam, and a pattern of holes. Examples of surface morphology in each observed regime are shown in Fig. 1. The holes were observed at the transition between parallel- and perpendicular-mode ripples. The first wavelengths to appear are reported in Table I. With the exception of the starred data points, which have entered the nonlinear regime and display increased roughness values, the parallel-mode ripple data follow an inverse wavelength/angle trend. This observation is consistent with the parallel-mode ripple data reported for Ar⁺ on Si.⁶ Perpendicular-mode wavelengths do not appear to vary significantly with angle or energy over the small range in this study.

We show in Fig. 2 the phase diagram of observed patterns as we vary the control parameters of ion energy versus incidence angle. Qualitatively, patterns at 250 and 500 eV were equivalent. Between incidence angles θ of 0° and 50°, flat, stable surfaces (smoothening) were observed. The RMS roughness of bare Ge was measured to be 0.162 nm. Final RMS roughness values of irradiated samples for $\theta < 55^\circ$ had an average roughness of 0.109 nm. Samples near the bifurcation^{17,21}—the transition between smooth and rippled surfa-

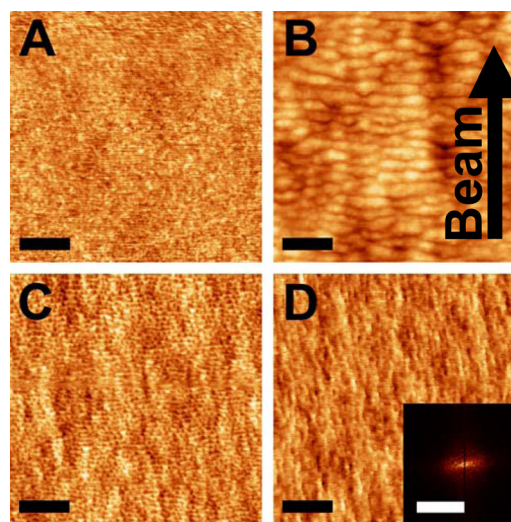


FIG. 1. (Color online) AFM images of Ge samples in the various morphological regimes. Samples were irradiated with different ion incidence angles at 250 eV at fluences of 4.5×10^{18} ions/cm² reckoned in a plane perpendicular to the ion beam. The projected ion beam direction is from the bottom to the top of the page. Scale bar lengths are 200 nm for AFM images, and $100 \mu\text{m}^{-1}$ for the FFT inset. Ion incidence angles, resulting surface morphologies, and height scales are (a) 5°, smooth, 1 nm, (b) 60°, parallel-mode ripples, 6 nm, (c) 75°, holes, 4 nm, and (d) 80°, perpendicular-mode ripples, 2 nm. Inset: FFT of image D, showing the emergence of perpendicular-mode ripples.

ces—at $\theta = 55^\circ$ showed increased final roughness values at an average of 0.174 nm with no detectable surface structures in both real and Fourier space. Between 60° and 70°, we observed parallel-mode ripples, in which the wave vector is parallel to the projection of the ion beam on the surface. At $\theta = 75^\circ$, holes were observed, which we interpret as the superposition of parallel- and perpendicular-mode ripples. Above the transition between parallel- and perpendicular-mode ripples at 75°, we observed perpendicular-mode ripples, in which the wave vector is perpendicular to the ion beam.

A time series study of pattern amplitude was conducted for the particular case of 500 eV Kr⁺ irradiation at 60° incidence (parallel-mode ripples). Samples were irradiated for durations ranging from 30 s to 10 min. RMS measurements

TABLE I. Wavelengths of pattern formation in linear regime, as measured with FFT.

Energy (eV)	Angle (°)	Mode	Wavelength (nm)
250	60		48 ± 6
250	70		27 ± 5
250	75		19 ± 2
250	75	⊥	21 ± 3
250	80	⊥	22 ± 4
500	60		35 ± 8
500	65		45 ± 7^a
500	70		35 ± 5^a
500	75		26 ± 4
500	75	⊥	23 ± 4

^aSamples that have started to enter the nonlinear regime of roughening, as indicated by significant increases in their measured RMS roughness.

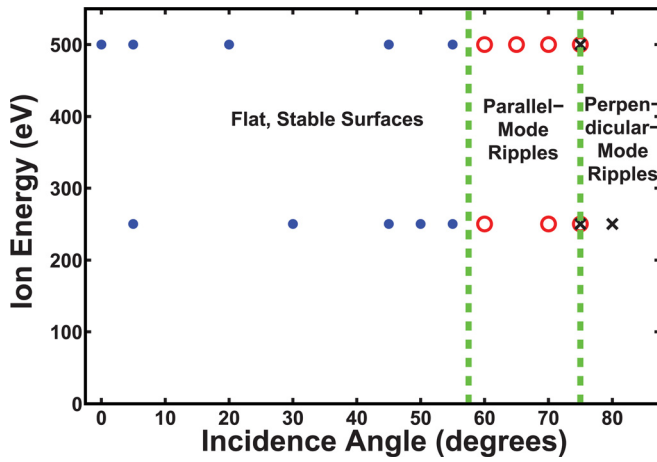


Fig. 2. (Color online) Pattern formation phase diagram. Qualitative patterning behavior is equivalent for both 250 and 500 eV ion energy. Filled circles: smoothing; open circles: parallel-mode ripples; crosses: perpendicular-mode ripples. Superposed circles and crosses indicate a hole pattern, which we interpret as the superposition of parallel- and perpendicular-mode ripples.

indicate that at this angle, amplitude saturation becomes significant after roughly 60 s of irradiation. Results reported in this paper, except where stated otherwise, are for the presaturation linear regime of exponential amplification or decay.

The behavior we observed for Kr⁺ on Ge is qualitatively similar to the response of Si to Ar⁺ irradiation, but there is a significant quantitative difference: whereas the bifurcation angle for Ar⁺ on Si was between 45° and 50°, for Kr⁺ on Ge it is between 55° and 60°.

Our findings are in marked contrast with the observations of noble gas ion-irradiated Ge, which are presented by Ziberi *et al.*¹⁵ At a Xe⁺ ion energy of 500 eV and at incidence angles of 0°, 5°, and 20°, Ziberi *et al.* report hillock structures, perpendicular mode ripples, and parallel-mode ripples, respectively, and they state that similar results were obtained for Kr⁺-irradiated Ge. Similarly, Carbone *et al.*²² report, for 1 keV Xe⁺-irradiated Ge at 10° incidence, dots evolving into parallel-mode ripples. In direct contrast to the results of Ziberi *et al.*, we observed smoothing for Kr⁺-irradiated Ge at all angles up to 57.5°. However, a subsequent paper by Ziberi and coauthors reports that patterns observed for low-energy, near-normal incidence bombardment of Si by Kr⁺ ions, despite being originally attributed to impurity-free ion bombardment, were actually a result of simultaneous sputter deposition of stainless steel.²³ While their contamination paper does not specifically discuss their prior work on Ge pattern formation, their original Kr⁺ on Si work was conducted using the same chamber, ion source, and experimental setup as their Kr⁺ on Ge work. Thus, the presence of impurities in their Kr⁺ on Si system suggests that their prior experiments with Kr⁺-irradiated Ge may also have incorporated impurities from the stainless steel chamber. In contrast, the experimental system used in this paper is identical to that used by Madi *et al.*, which has been shown to avoid metallic impurity incorporation.⁶ Thus, the difference in metallic impurity incorporation explains the contrast between our results and those of Ziberi *et al.*¹⁵

Most theories of surface morphology evolution under ion irradiation develop a partial differential equation (PDE) for the temporal evolution of the surface height $h(x,y,t)$. Here x is the direction of the projection of the ion beam along the surface of average orientation, y is the direction in this surface perpendicular to x , and h is measured along the z direction, which is perpendicular to both x and y , and sputter erosion causes the surface average of $\partial h(x,y,t)/\partial t$ to be negative. The surface of an initially flat, monatomic, isotropic solid undergoing uniform ion irradiation evolves, during the linear regime at early time and low fluence, according to¹⁷

$$\frac{\partial h(x,y,t)}{\partial t} = -I + \{S_X \partial_{XX} + S_Y \partial_{YY} - B \nabla^4\} h,$$

where $I(\theta)$ is the average vertical erosion rate; $S_X(\theta)$ and $S_Y(\theta)$ are the curvature coefficients for parallel and perpendicular modes, respectively; and B is the coefficient describing surface relaxation via surface diffusion^{5,24} or surface-confined viscous flow.^{17,25,26} The second-derivative terms are stabilizing when the curvature coefficients are positive, and they are destabilizing when curvature coefficients are negative. Writing the surface topography as a sum of normal modes of wave vector \mathbf{q} , $h(\mathbf{q}, t) \propto e^{w(\mathbf{q})t} e^{i(q_x x + q_y y)}$, and inserting this into the PDE results in the linear dispersion relation

$$R(\mathbf{q}) = -S_X q_x^2 - S_Y q_y^2 - B(q_x^2 - q_y^2)^2,$$

where $R(\mathbf{q}) \equiv \text{Re}(\omega(\mathbf{q}))$. In principle, linear stability analyses of both erosive effects and redistributive effects yield contributions $S^{\text{eros}}(\theta)$ and $S^{\text{redist}}(\theta)$, respectively, to the curvature coefficients in each direction. BH theory assumes that the entire contribution is from erosion, whereas the CV model¹⁶ assumes that the entire contribution is redistributive. BH theory predicts that the surface is linearly unstable to some wavevector at all incidence angles, including near-normal incidence, in direct contrast to our experimental results, which show smoothing at all angles less than 57.5°. The CV model assumes that the net effect of the ion impact-induced collision cascade is embodied in the average vector sum of the displacements of all recoiled atoms, which is an atomic displacement vector directed parallel to the incident ion beam and of angle-independent magnitude δ . The effect of the collision cascade on the surface is then assumed to be the projection of this net displacement vector along the surface. This simple model for the incidence-angle dependence of the redistribution, as well as the incidence-angle dependence of the flux dilution, does not vary with energy or ion or target masses. Expanding the expression for this surface-projected flux to first order in spatial derivatives yields an expression for the mass redistribution-driven curvature coefficient in the x -direction ($S_X^{\text{redist}}(\theta) = J \delta \Omega \cos(2\theta)$), where J is the ion flux and Ω is the atomic volume, that is stabilizing at low incidence angles and destabilizing at higher incidence angles. Although this switch from stability to instability with increasing θ is qualitatively consistent with our experimental results, this simple model of mass redistribution always predicts a stability/instability bifurcation at $\theta = 45^\circ$ in both its

original form and as modified by Madi and Aziz.¹⁷ Whereas this prediction is close to the value of $\theta = 48^\circ$ observed for Ar⁺ bombardment of Si, there is a significant discrepancy with the bifurcation angle of $57.5^\circ \pm 2.5^\circ$ that we report here for Kr⁺ bombardment of Ge, and thus the CV model cannot fully explain our results.

The crater-function theory of Norris *et al.* allows both erosive and redistributive contributions to the curvature coefficients to be evaluated on equal footing and compared, and has the potential to explain the observed value of the transition angle in the Kr⁺ on Ge system. It takes as input the shape of the average impact crater, and its dependence on incidence angle, which has been evaluated for Ar⁺ on Si in molecular dynamics (MD) using a widely used classical Hamiltonian.⁷ The theory contains no adjustable parameters—the only parameters reside in the interaction Hamiltonian, and these were not adjusted to fit topography evolution experiments. In the case of Ar⁺ bombardment of Si, Norris theory on the existing MD predicts a stability/instability bifurcation at $\theta = 38^\circ$, which is about 10° smaller than the experimental value. Currently, it is not clear whether this discrepancy reflects a shortcoming in the classical Hamiltonian or in Norris theory itself. In order to quantitatively test Norris theory for Kr⁺ on Ge, we would first require MD simulations to quantify the θ -dependence of the average impact-induced crater. Our results do not appear to be fundamentally inconsistent with Norris theory, and this remains an avenue for future research.

We also observed experimentally that amplification rates of the parallel-mode ripples increase as the incidence angle is moved away from the observed bifurcation angle of 57.5° . Irradiation at 500 eV and 60° for 60 s resulted in a measured RMS roughness of 0.26 nm, whereas irradiation at the same energy for the same duration at 70° resulted in an RMS roughness value of 1.02 nm. As θ was increased from 60° to 70° , roughness increased while the areal density (reckoned in a plane parallel to the surface) of surface ion impacts decreased: an RMS value of 0.42 nm was recorded for a 60° sample with an impact density of 3.6×10^{17} impacts/cm² (4 min bombardment), an RMS roughness of 2.03 nm was recorded for a 65° sample with 2.3×10^{17} impacts/cm² (3 min bombardment), and an RMS roughness of 2.30 nm was observed for bombardment at 70° with an impact density of 1.8×10^{17} impacts/cm² (3 min bombardment). The inverse relationship between roughness and ion impact density for these samples indicates that roughening occurs more rapidly as incidence angle increases away from the bifurcation point, up to an angle of maximum roughening rate at $\theta \sim 70^\circ$. This observation implies that the destabilizing influence of an individual ion impact ($S_X(\theta)$) increases more rapidly than the areal density of ion impacts decreases with increasing incidence angle. Furthermore, we observed increased surface roughness with increasing θ in the smoothening regime at 55° , near the bifurcation between 55° and 60° . To discover whether this roughness increase is the beginning of pattern formation, we irradiated a sample at $\theta = 55^\circ$ for 25 min at 500 eV and observed no discernible ripple or hole patterns in real or Fourier space. Thus, it would appear that the increased

roughness is a result of proximity to the bifurcation between smoothness and parallel-mode ripples.

Our observations of small-amplitude ripple pattern formation at the relatively low energies of 250 and 500 eV contrast with the high aspect ratio, finger-like structures observed when Ge is irradiated with ions of several tens of keV to MeV energies.^{9–13} Our topographies are much more similar to those observed for low energy Ar⁺ on Si.⁶ This suggests that fundamentally different processes control topography evolution under low-energy and high-energy ion irradiation, which remains an avenue for future research.

IV. SUMMARY AND CONCLUSIONS

In conclusion, smoothening, parallel-mode ripples, and perpendicular-mode ripples are observed as the deviation from normal incidence is increased, independent of ion energy. The phase diagram is inconsistent with that of Ziberi *et al.* under nominally identical conditions and is qualitatively similar to the results of Madi *et al.* on Ar⁺-irradiated Si. Whereas the modified CV mass redistribution model explained silicon behavior quantitatively,¹⁷ albeit with an adjustable parameter, the higher bifurcation angle observed in the present study of Kr⁺ on Ge indicates that more nuanced theoretical approaches are necessary. A priority for future research is the extension of crater function theory to the Kr⁺ on Ge system in order to determine whether its predictions are consistent with these experimental results.

ACKNOWLEDGMENTS

The authors would like to acknowledge Leszek Wielunski of Rutgers University for RBS measurements of impurity concentrations in the samples used in this study. They would also like to acknowledge Eitan Anzenberg and Karl F. Ludwig, Jr. of Boston University for helpful discussions. This research was supported by DOE Grant DE-FG-02-06ER46335. The work was performed in part at the Center for Nanoscale Systems (CNS), a member of the National Nanotechnology Infrastructure Network (NNIN), which is supported by the National Science Foundation under NSF Award No. ECS-0335765. CNS is part of Harvard University.

¹M. Moseler, P. Gumbsch, C. Casiraghi, A. C. Ferrari, and J. Robertson, *Science* **309**, 1545 (2005).

²Q. Wei, J. Lian, S. Zhu, W. Li, K. Sun, and L. Wang, *Chem. Phys. Lett.* **452**, 124 (2008).

³A. Cuenat, H. B. George, K. C. Chang, J. Blakely, and M. J. Aziz, *Adv. Mater.* **17**, 2845 (2005).

⁴P. Sigmund, *J. Mater. Sci.* **8**, 1545 (1973).

⁵R. M. Bradley and J. M. Harper, *J. Vac. Sci. Technol. A* **6**, 2390 (1988).

⁶C. S. Madi and M. J. Aziz, *Appl. Surf. Sci.* **258**, 4112 (2011).

⁷S. A. Norris, J. Samela, L. Bukonte, M. Backman, F. Djurabekova, K. Nordlund, C. S. Madi, M. P. Brenner, and M. J. Aziz, *Nat. Commun.* **2**, 276 (2011).

⁸S. A. Norris, M. P. Brenner, and M. J. Aziz, *J. Phys.: Condens. Matter* **21**, 224017 (2009).

⁹Q. Wei, X. Zhou, B. Joshi, Y. Chen, K.-D. Li, Q. Wei, K. Sun, and L. Wang, *Adv. Mater.* **21**, 2865 (2009).

¹⁰I. H. Wilson, *J. Appl. Phys.* **53**, 1698 (1982).

¹¹W. Zhou, A. Cuenat, and M. J. Aziz, *Microscopy of Semiconducting Materials 2003: Proceedings of the 13th International Conference on*

- Microscopy of Semiconducting Materials*, edited by A. G. Cullis and P. A. Midgley (Cambridge University, 2003).
- ¹²S. Ichim and M. J. Aziz, *J. Vac. Sci. Technol. B* **23**, 1068 (2005).
- ¹³M. Kolíbal, T. Matlocha, T. Vystavěl, and T. Šikola, *Nanotechnology* **22**, 105304 (2011).
- ¹⁴M. Fritzsche, A. Muecklich, and S. Facsko, *Appl. Phys. Lett.* **100**, 223108 (2012).
- ¹⁵B. Ziberi, M. Cornejo, F. Frost, and B. Rauschenbach, *J. Phys.: Condens. Matter* **21**, 224003 (2009).
- ¹⁶G. Carter and V. Vishnyakov, *Phys. Rev. B* **54**, 17647 (1996).
- ¹⁷C. S. Madi, E. Anzenberg, K. F. Ludwig, and M. J. Aziz, *Phys. Rev. Lett.* **106**, 066101 (2011).
- ¹⁸C. S. Madi, "Linear stability and instability patterns in ion bombarded silicon surfaces," Ph.D. thesis (Harvard University, 2011).
- ¹⁹C. S. Madi, B. Davidovitch, H. B. George, S. A. Norris, M. P. Brenner, and M. J. Aziz, *Phys. Rev. Lett.* **101**, 246102 (2008).
- ²⁰I. Horcas, R. Fernandez, J. M. Gomez-Rodriguez, J. Colchero, J. Gomez-Herrero, and A. M. Baro, *Rev. Sci. Instrum.* **78**, 013705 (2007).
- ²¹P. Karmakar, S. A. Mollick, D. Ghose, and A. Chakrabarti, *Appl. Phys. Lett.* **93**, 103102 (2008).
- ²²D. Carbone, A. Alija, O. Plantevin, R. Gago, S. Facsko, and T. H. Metzger, *Nanotechnology* **19**, 035304 (2008).
- ²³S. Macko, F. Frost, B. Ziberi, D. F. Forster, and T. Michely, *Nanotechnology* **21**, 085301 (2010).
- ²⁴W. W. Mullins, *J. Appl. Phys.* **30**, 77 (1959).
- ²⁵S. E. Orchard, *Appl. Sci. Res., Sect. A* **11**, 451 (1963).
- ²⁶C. C. Umbach, R. L. Headrick, and K. C. Chang, *Phys. Rev. Lett.* **87**, 246104 (2001).